2024 IEEE 63rd Conference on Decision and Control (CDC)
December 16-19, 2024. MiCo, Milan, Italy

Immersion and Invariance Design for Adaptive Longitudinal Vehicles Platooning

Di Liu, *Member, IEEE*, Simone Baldi, *Senior Member, IEEE*, Alessandro Astolfi, *Fellow, IEEE*

***Abstract*— This work shows how widely adopted longitudinal platooning protocols can be made adaptive via an immersion and invariance (I&I) approach. Such an I&I approach advances the state of the art on adaptive longitudinal platooning, which mostly relies on model reference adaptive control, while also extending the standard I&I design by compensating for exogenous effects from the preceding vehicle in the adaptive law. Two I&I designs are presented and compared with the corresponding state-of-the-art model reference adaptive control designs to demonstrate their effectiveness.**

I. Introduction

Longitudinal platooning refers to formations of automated vehicles with control protocols that use feedback from on-board sensing (radar, tachometer, accelerometer, etc.) and inter-vehicle wireless communication to keep a desired distance. The name Cooperative Adaptive Cruise Control (CACC) is nowadays standard to indicate several such protocols [1]. Historically, the term 'adaptive' was introduced in Adaptive Cruise Control (ACC), the technology prior to CACC only relying on on-board sensing, to indicate a cruise control that could adapt to different speeds of the preceding vehicle. As such, the term 'adaptive' in ACC/CACC is not used in the same sense as in 'adaptive control': evidence of this is that standard longitudinal platooning protocols are not designed using adaptive control. Yet, as the time constants of the vehicles composing the platoon are hardly known in practice [2]–[4], embedding longitudinal platooning with adaptive control capabilities is practically relevant.

While it might be difficult, if at all possible, to categorize all longitudinal platooning protocols in the literature, we focus on two rather standard protocols: chronologically, [5] was probably the first protocol with a string stability analysis under constant time headway, showing improved disturbance rejection as compared to constant distance headway. Several studies have been conducted on this protocol, such as [4], [6], [7], making it one of the most popular. As the understanding of longitudinal platooning improved, a new protocol was later developed from the perspective of disturbance decoupling [8]. Such a perspective is particularly useful in longitudinal platooning as it guarantees string stability under constant time headway as a by-product, giving a new insight into longitudinal platooning [9], [10].

Alternative approaches, such as protocols based on consensus or energy damping [11], [12], have been proposed. We focus on the protocols stemming from [5], [8] due to their string stability property under constant time headway and due to the existing adaptive control mechanisms proposed for these protocols, namely, [13], [14] for the protocol in [5], and [15], [16] for the protocol in [8]. The interested reader can verify that such adaptation mechanisms rely on model reference adaptive control (MRAC). This note shows how, for the aforementioned widely adopted longitudinal platooning protocols, new adaptation mechanisms can be designed using an immersion and invariance (I&I) approach. I&I is a tool introduced in [17] for the (adaptive) stabilization of nonlinear systems. Over the years, I&I has been exploited for observer design [18], [19], adaptive control for classes of nonlinearly parametrized systems [20], contraction and input-to-state stability designs [21], [22], and orbital stabilization [23]. Despite the progress, the application of I&I to longitudinal platooning requires peculiar features: as a matter of fact, the I&I designs in this work extend the standard I&I design by compensating for exogenous effects from the preceding vehicle in the adaptive law.

The rest of the paper is organized as follows: two widely adopted longitudinal platooning protocols are presented in Sect. II (first the one in [8], then the one in [5]), and the corresponding I&I designs are presented and analyzed in Sect. III and IV, respectively. Comparisons with the corresponding state-of-the-art MRAC designs are presented in Sect. V, with conclusions in Sect. VI.

II. Baseline protocols and problem statement

As customary in the literature [4], [11], [24], we introduce longitudinal platooning via a pair of predecessor-follower vehicles (see Fig. 1) indexed as $i-1$ and i, respectively, yielding the equations

$$\begin{aligned} &\dot{s}_i(t)=v_i(t), && \dot{s}_{i-1}(t)=v_{i-1}(t),\\ &\dot{v}_i(t)=a_i(t), && \dot{v}_{i-1}(t)=a_{i-1}(t),\\ &\tau_i\dot{a}_i(t)=-a_i(t)+u_i(t), && \tau_{i-1}\dot{a}_{i-1}(t)=-a_{i-1}(t)+u_{i-1}(t), \end{aligned} \tag{1}$$

where s_i, v_i, a_i are the longitudinal position, velocity, and acceleration of vehicle i (similar for vehicle $i-1$). The input u_i is a desired acceleration passing through a first-order filter with time constant $\tau_i > 0$, representing the time needed by

This research was partly supported by Horizon Europe Marie Sklodowska-Curie Action no. 101146446, by UKRI Research and Innovation no. EP/Z002214/1, by Natural Science Foundation of China grants 62073074 and 62233004, and by Jiangsu Provincial Scientific Research Center of Applied Mathematics grant BK20233002.

D. Liu is with Department of Electrical and Electronic Engineering, Imperial College London, UK, (di.liu@imperial.ac.uk)
S. Baldi is with School of Mathematics, Southeast University, China (simonebaldi@seu.edu.cn)
A. Astolfi is with Department of Electrical and Electronic Engineering, Imperial College London, UK, and also with Dipartimento di Ingegneria Civile e Ingegneria Informatica, Università di Roma "Tor Vergata", Via del Politecnico, Italy (a.astolfi@imperial.ac.uk)

a_i to reach u_i, due to the powertrain/braking dynamics. This time constant is affected by vehicle mass, road slope, gear, among other factors, hence it is often *unknown* in practice.

Longitudinal platooning is established through the spacing error and the relative velocity, defined as

$$\begin{aligned} e_i(t) &= s_{i-1}(t) - s_i(t) - hv_i(t), \\ \nu_i(t) &= v_{i-1}(t) - v_i(t), \end{aligned} \tag{2}$$

where $h > 0$ is a time headway to represent typical driving behavior of increasing the inter-vehicle distance as the velocity increases [1], [8], [25]. We now recall two longitudinal platooning protocols commonly adopted in the literature.

A. Baseline non-adaptive platooning protocols

The longitudinal platooning protocol introduced in [8] in the framework of disturbance decoupling is described by the equation

$$u_i(t) = \theta_1 e_i(t) + \theta_2 \nu_i(t) + (1 - \frac{\tau_i}{h} - h\theta_2)a_i(t) + \frac{\tau_i}{h}a_{i-1}(t), \tag{3}$$

for arbitrary $\theta_1 > 0$ and $\theta_2 > 0$. One can recognize a proportional-derivative feedback from e_i and $\dot{e}_i = \nu_i - ha_i$, and a term proportional to the relative acceleration. Feedback from e_i, $\dot{e}_i$, and a_i can be obtained from on-board sensing, like radar, tachometer and accelerometer, while feedback from a_{i-1} requires inter-vehicle wireless communication, in line with the cooperative adaptive cruise control (CACC) technology [1].

Another longitudinal platooning protocol, introduced in [5], uses additional dynamics for u_i, described by

$$h\dot{u}_i(t) = -u_i(t) + \theta_1 e_i(t) + \theta_2 \nu_i(t) - h\theta_2 a_i(t) + u_{i-1}(t), \tag{4}$$

with $\theta_1 > 0$ and $\theta_2 > 0$, such that $\theta_2 > \tau_i\theta_1$. One can again recognize a proportional-derivative feedback from e_i and $\dot{e}_i$, and feedback from u_{i-1} requiring inter-vehicle wireless communication. The protocols (3) and (4) have their own advantages and disadvantages. For example, (3) guarantees disturbance decoupling even with heterogeneous $\tau_{i-1} \neq \tau_i$, but requires exact knowledge of τ_i; on the other hand, (4) guarantees disturbance decoupling only for homogeneous $\tau_{i-1} = \tau_i$, but the inequality $\theta_2 > \tau_i\theta_1$ relaxes the exact knowledge of τ_i. The interested reader is referred to the literature for a detailed set of properties of the two protocols.

B. Control problem

As both protocols (3) and (4) cannot handle large uncertainty in the vehicle time constants, an adaptive longitudinal platooning problem is formulated as follows.

Control Problem: Consider the predecessor-follower model (1) with spacing error (2). Design an adaptive controller u_i such that, for any unknown $\tau_i > 0$ and $\tau_{i-1} > 0$, and any bounded $a_{i-1}(\cdot)$ and $u_{i-1}(\cdot)$, it holds that

$$\lim_{t\to\infty} e_i(t) = 0. \tag{5}$$

The rationale for considering bounded $a_{i-1}(\cdot)$, $u_{i-1}(\cdot)$, is that these terms enter as exogenous disturbances in the error dynamics. For the protocol (3) this can be seen by writing

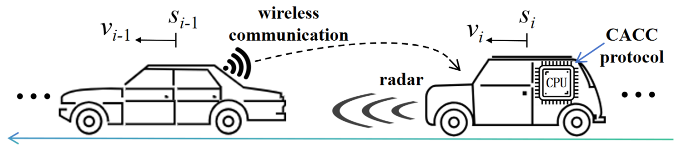

Fig. 1: Predecessor and follower in a longitudinal platoon.

$$\begin{bmatrix} \dot{e}_i \\ \dot{\nu}_i \\ \dot{a}_i \end{bmatrix} = \begin{bmatrix} 0 & 1 & -h \\ 0 & 0 & -1 \\ 0 & 0 & -\frac{1}{\tau_i} \end{bmatrix} \begin{bmatrix} e_i \\ \nu_i \\ a_i \end{bmatrix} + \begin{bmatrix} 0 \\ 0 \\ \frac{1}{\tau_i} \end{bmatrix} u_i + \begin{bmatrix} 0 \\ 1 \\ 0 \end{bmatrix} a_{i-1}. \tag{6}$$

Analogously, for the protocol (4), we obtain

$$\begin{bmatrix} \dot{e}_i \\ \dot{\nu}_i \\ \dot{a}_i \\ \dot{u}_i \end{bmatrix} = \begin{bmatrix} 0 & 1 & -h & 0 \\ 0 & 0 & -1 & 0 \\ 0 & 0 & -\frac{1}{\tau_i} & \frac{1}{\tau_i} \\ \frac{\theta_1}{h} & \frac{\theta_2}{h} & -\theta_2 & -\frac{1}{h} \end{bmatrix} \begin{bmatrix} e_i \\ \nu_i \\ a_i \\ u_i \end{bmatrix} + \begin{bmatrix} 0 \\ 0 \\ \frac{1}{\tau_i} \\ 0 \end{bmatrix} \Delta u_i + \begin{bmatrix} 0 & 0 \\ 1 & 0 \\ 0 & 0 \\ 0 & \frac{1}{h} \end{bmatrix} \begin{bmatrix} a_{i-1} \\ u_{i-1} \end{bmatrix}, \tag{7}$$

where Δu_i has been introduced as the adaptive input to be designed.

III. First Immersion and Invariance design

We now discuss how the protocol (3) can be made adaptive. Let $\tau_m > 0$ be a target time constant. Because $\theta_1 > 0$ and $\theta_2 > 0$ in (3) can be arbitrary, define, without loss of generality the control

$$u_i = a_i + \tau_i \left(\frac{\theta_1}{\tau_m} e_i + \frac{\theta_2}{\tau_m} \nu_i - \left(\frac{h\theta_2}{\tau_m} + \frac{1}{h} \right) a_i + \frac{1}{h} a_{i-1} \right), \tag{8}$$

satisfying the same properties as (3). Note that (8) is linearly parametrized with respect to the unknown τ_i. Using the target time constant τ_m, define the target dynamics

$$\begin{bmatrix} \dot{\bar{e}}_i \\ \dot{\bar{\nu}}_i \\ \dot{\bar{a}}_i \end{bmatrix} = \underbrace{\begin{bmatrix} 0 & 1 & -h \\ 0 & 0 & -1 \\ \frac{\theta_1}{\tau_m} & \frac{\theta_2}{\tau_m} & -\frac{h\theta_2}{\tau_m} - \frac{1}{h} \end{bmatrix}}_{A_m} \underbrace{\begin{bmatrix} \bar{e}_i \\ \bar{\nu}_i \\ \bar{a}_i \end{bmatrix}}_{\bar{x}} + \underbrace{\begin{bmatrix} 0 \\ 1 \\ \frac{1}{h} \end{bmatrix}}_{G_m} a_{i-1}, \tag{9}$$

that arise from controlling the dynamics (6) with the ideal controller (8). Adding and subtracting the ideal controller (8) from (6) allows writing the actual dynamics as

$$\begin{aligned} \begin{bmatrix} \dot{e}_i \\ \dot{\nu}_i \\ \dot{a}_i \end{bmatrix} &= \begin{bmatrix} 0 & 1 & -h \\ 0 & 0 & -1 \\ \frac{\theta_1}{\tau_m} & \frac{\theta_2}{\tau_m} & -\frac{h\theta_2}{\tau_m} - \frac{1}{h} \end{bmatrix} \underbrace{\begin{bmatrix} e_i \\ \nu_i \\ a_i \end{bmatrix}}_{x} + \begin{bmatrix} 0 \\ 1 \\ \frac{1}{h} \end{bmatrix} a_{i-1} + \underbrace{\begin{bmatrix} 0 \\ 0 \\ \frac{1}{\tau_i} \end{bmatrix}}_{g} \tilde{u}_i \\ &\quad - \begin{bmatrix} 0 \\ 0 \\ \frac{1}{\tau_i} \end{bmatrix} \tau_i \underbrace{\left(\frac{\theta_1}{\tau_m} e_i + \frac{\theta_2}{\tau_m} \nu_i - \left(\frac{h\theta_2}{\tau_m} + \frac{1}{h} \right) a_i + \frac{1}{h} a_{i-1} \right)}_{\psi}, \end{aligned} \tag{10}$$

where we have defined $\tilde{u}_i = u_i - a_i$ for compactness. Subtracting the actual dynamics (10) and the ideal target dynamics (9) gives

$$\begin{bmatrix} \dot{\tilde{e}}_i \\ \dot{\tilde{\nu}}_i \\ \dot{\tilde{a}}_i \end{bmatrix} = \begin{bmatrix} 0 & 1 & -h \\ 0 & 0 & -1 \\ \frac{\theta_1}{\tau_m} & \frac{\theta_2}{\tau_m} & -\frac{h\theta_2}{\tau_m} - \frac{1}{h} \end{bmatrix} \begin{bmatrix} \tilde{e}_i \\ \tilde{\nu}_i \\ \tilde{a}_i \end{bmatrix} + \begin{bmatrix} 0 \\ 0 \\ \frac{1}{\tau_i} \end{bmatrix} \tilde{u}_i - \begin{bmatrix} 0 \\ 0 \\ \frac{1}{\tau_i} \end{bmatrix} \psi\tau_i, \tag{11}$$

where $\tilde{e}_i = e_i - \bar{e}_i$, $\tilde{v}_i = v_i - \bar{v}_i$, $\tilde{a}_i = a_i - \bar{a}_i$. Let $\tilde{x} = x - \bar{x}$, with x as in (10) and $\bar{x}$ as in (9). The following result holds.

Theorem 1. *The predecessor-follower dynamics (11) are adaptively stabilizable via immersion and invariance (I&I). An I&I design is given by the adaptive law*

$$\dot{\hat{\tau}}_i(t) = -\frac{\partial \beta}{\partial \tilde{x}} A_{\mathrm{m}} \tilde{x}(t) - \frac{\partial \beta}{\partial \bar{x}} \left(A_{\mathrm{m}} \bar{x}(t) + G_{\mathrm{m}} a_{i-1}(t) \right), \tag{12}$$

with the control law

$$u_i(t) = a_i(t) + \psi(t) \left(\hat{\tau}_i(t) + \beta(\tilde{x}(t), \bar{x}(t)) \right), \tag{13}$$

and

$$\beta(\tilde{x}, \bar{x}) = -\gamma \tilde{a}_i \left[\frac{\theta_1}{\tau_{\mathrm{m}}} e_i + \frac{\theta_2}{\tau_{\mathrm{m}}} v_i + \frac{1}{h} a_{i-1} - \left(\frac{\tilde{a}_i}{2} + \bar{a}_i \right) \left(\frac{h\theta_2}{\tau_{\mathrm{m}}} + \frac{1}{h} \right) \right], \tag{14}$$

with $\gamma > 0$.

Proof. Stabilizability via immersion and invariance requires to verify a set of conditions, see [17]. Because the stability of the target system (9), the immersion condition, and the implicit manifold condition follow almost directly from [17], we focus on the condition of manifold attractivity and trajectory boundedness. This condition requires to prove that all trajectories of the system

$$\begin{aligned} \dot{\tilde{x}}(t) &= A_{\mathrm{m}} \tilde{x}(t) + g \psi(x(t)) z(t) \\ \dot{z}(t) &= \left[\frac{\partial \beta}{\partial \tilde{x}} g \psi(x(t)) \right] z(t), \end{aligned} \tag{15}$$

are bounded and satisfy the condition $\lim_{t \to \infty} \tilde{x}(t) = 0$. To this end note that the dynamics of $\tilde{x}$ can be calculated as

$$\begin{aligned} \dot{\tilde{x}}(t) &= A_{\mathrm{m}} \tilde{x}(t) + g \tilde{u}_i(t) - g \psi(t) \tau_i \\ &= A_{\mathrm{m}} \tilde{x}(t) + g \psi(t) z(t), \end{aligned} \tag{16}$$

where we have used the off-manifold variable $z = \hat{\tau}_i - \tau_i + \beta(\tilde{x}, \bar{x})$ and the controller in the form $\tilde{u}_i = \psi(\hat{\tau}_i + \beta(\tilde{x}, \bar{x}))$. The dynamics of z can be calculated as

$$\begin{aligned} \dot{z}(t) = \dot{\hat{\tau}}_i(t) + \frac{\partial \beta}{\partial \tilde{x}} \dot{\tilde{x}}(t) + \frac{\partial \beta}{\partial \bar{x}} \dot{\bar{x}}(t) = \dot{\hat{\tau}}_i(t) + \\ \frac{\partial \beta}{\partial \tilde{x}} \left(A_{\mathrm{m}} \tilde{x}(t) + g \psi(t) z(t) \right) + \frac{\partial \beta}{\partial \bar{x}} \left(A_{\mathrm{m}} \bar{x}(t) + G_{\mathrm{m}} a_{i-1}(t) \right). \end{aligned} \tag{17}$$

Choosing the adaptive law (12), the z dynamics in (15) are obtained. To prove boundedness of the trajectories in (15), consider the Lyapunov function

$$W(\tilde{x}, z) = \tilde{x}^\top \frac{P}{2} \tilde{x} + \frac{\rho}{2} z^\top z, \tag{18}$$

with $\rho > 0$, and $P > 0$ solution to the Lyapunov equation

$$P A_{\mathrm{m}} + A_{\mathrm{m}}^\top P + Q = 0, \quad Q > 0. \tag{19}$$

The time derivative of the Lyapunov function along the trajectories of the system gives

$$\dot{W} = \tilde{x}^\top \frac{P A_{\mathrm{m}} + A_{\mathrm{m}}^\top P}{2} \tilde{x} + \tilde{x}^\top P g \psi z + \rho z^\top \frac{\partial \beta}{\partial \tilde{x}} g \psi z. \tag{20}$$

Peter-Paul inequality applied to the second term in (20) gives

$$\tilde{x}^\top P g \psi z \le \frac{\tilde{x}^\top P g g^\top P \tilde{x}}{2\alpha} + \frac{\alpha}{2} z^\top \psi \psi^\top z, \tag{21}$$

for any $\alpha > 0$. Using the fact that β in (14) is such that

$$\frac{\partial \beta}{\partial \tilde{x}} g = -\frac{\gamma}{\tau_i} \psi, \tag{22}$$

we obtain

$$\dot{W} \le -\tilde{x}^\top \frac{Q}{2} \tilde{x} + \frac{\tilde{x}^\top P g g^\top P \tilde{x}}{2\alpha} + z^\top \psi \left(\frac{\alpha}{2} - \rho \frac{\gamma}{\tau_i} \right) \psi^\top z, \tag{23}$$

which is negative semidefinite for $\rho > \alpha \tau_i / (2\gamma)$ and α sufficiently large. This results in boundedness of all trajectories of (15). Convergence of $\tilde{x}$ is established using Barbalat's Lemma. Having established all conditions for stabilizability via I&I, we finally verify (5) by writing $e_i = \bar{e}_i + \tilde{e}_i$, where $\bar{e}_i$ convergences to zero due to the disturbance decoupling property of the ideal closed loop (9), whereas convergence of $\tilde{e}_i$ has been proven via Lyapunov analysis. This concludes the proof. ■

As compared to the standard I&I design [17], the proposed I&I design considers exogenous terms. To tackle these exogenous effects, coming from the preceding vehicle, new terms have been included in the adaptive law (12).

The adaptive law (12) exploits what is known in I&I literature as *realizability* of the target dynamics [17, Sect. IV-D]. Being based on a target time constant τ_{m} chosen by the designer, the target dynamics are realizable, i.e., independent of the unknown parameters. Such a choice of the target dynamics is reminiscent of the reference dynamics in the MRAC design, which allows a direct comparison between the two approaches, as given in Sect. V.

IV. Second Immersion and Invariance design

We now discuss how the protocol (4) can be made adaptive. Analogous to the previous design, let $\tau_{\mathrm{m}} > 0$ represent a target time constant, chosen so that $\theta_2 > \tau_{\mathrm{m}} \theta_1$. Straightforward calculations show that the controller

$$\Delta u_i(t) = \left(\frac{\tau_i}{\tau_{\mathrm{m}}} - 1 \right) (u_i(t) - a_i(t)), \tag{24}$$

is stabilizing, and results in the target dynamics

$$\begin{bmatrix} \dot{\bar{e}}_i \\ \dot{\bar{v}}_i \\ \dot{\bar{a}}_i \\ \dot{\bar{u}}_i \end{bmatrix} = \underbrace{\begin{bmatrix} 0 & 1 & -h & 0 \\ 0 & 0 & -1 & 0 \\ 0 & 0 & -\frac{1}{\tau_{\mathrm{m}}} & \frac{1}{\tau_{\mathrm{m}}} \\ \frac{\theta_1}{h} & \frac{\theta_2}{h} & -\theta_2 & -\frac{1}{h} \end{bmatrix}}_{A_{\mathrm{m}}} \underbrace{\begin{bmatrix} \bar{e}_i \\ \bar{v}_i \\ \bar{a}_i \\ \bar{u}_i \end{bmatrix}}_{\bar{x}} + \underbrace{\begin{bmatrix} 0 & 0 \\ 1 & 0 \\ 0 & 0 \\ 0 & \frac{1}{h} \end{bmatrix}}_{G_{\mathrm{m}}} \begin{bmatrix} a_{i-1} \\ u_{i-1} \end{bmatrix}. \tag{25}$$

Adding and subtracting the ideal controller (24) from (7), we rewrite the actual dynamics as

$$\begin{aligned} \begin{bmatrix} \dot{e}_i \\ \dot{v}_i \\ \dot{a}_i \\ \dot{u}_i \end{bmatrix} &= \begin{bmatrix} 0 & 1 & -h & 0 \\ 0 & 0 & -1 & 0 \\ 0 & 0 & -\frac{1}{\tau_{\mathrm{m}}} & \frac{1}{\tau_{\mathrm{m}}} \\ \frac{\theta_1}{h} & \frac{\theta_2}{h} & -\theta_2 & -\frac{1}{h} \end{bmatrix} \underbrace{\begin{bmatrix} e_i \\ v_i \\ a_i \\ u_i \end{bmatrix}}_{x} + \begin{bmatrix} 0 & 0 \\ 1 & 0 \\ 0 & 0 \\ 0 & \frac{1}{h} \end{bmatrix} \begin{bmatrix} a_{i-1} \\ u_{i-1} \end{bmatrix} \\ &+ \begin{bmatrix} 0 \\ 0 \\ \frac{1}{\tau_i} \\ 0 \end{bmatrix} \Delta \tilde{u}_i - \begin{bmatrix} 0 \\ 0 \\ \frac{1}{\tau_i} \\ 0 \end{bmatrix} \tau_i \underbrace{\frac{u_i - a_i}{\tau_{\mathrm{m}}}}_{\psi}, \end{aligned} \tag{26}$$

where we have defined $\Delta\tilde{u}_i = \Delta u_i + u_i - a_i$ for compactness. By subtracting the actual and the ideal target dynamics (26) and (25), we obtain

$$\begin{bmatrix}\dot{\tilde{e}}_i\\ \dot{\tilde{v}}_i\\ \dot{\tilde{a}}_i\\ \dot{\tilde{u}}_i\end{bmatrix} = \begin{bmatrix}0 & 1 & -h & 0\\ 0 & 0 & -1 & 0\\ 0 & 0 & -\frac{1}{\tau_\mathrm{m}} & \frac{1}{\tau_\mathrm{m}}\\ \frac{\theta_1}{h} & \frac{\theta_2}{h} & -\theta_2 & -\frac{1}{h}\end{bmatrix}\begin{bmatrix}\tilde{e}_i\\ \tilde{v}_i\\ \tilde{a}_i\\ \tilde{u}_i\end{bmatrix} + \begin{bmatrix}0\\0\\\frac{1}{\tau_i}\\0\end{bmatrix}\Delta\tilde{u}_i + \begin{bmatrix}0\\0\\-\frac{1}{\tau_i}\\0\end{bmatrix}\psi\tau_i, \tag{27}$$

where $\tilde{e}_i = e_i - \bar{e}_i$, $\tilde{v}_i = v_i - \bar{v}_i$, $\tilde{a}_i = a_i - \bar{a}_i$, $\tilde{u}_i = u_i - \bar{u}_i$. Let $\tilde{x} = x - \bar{x}$, with x as in (26) and $\bar{x}$ as in (25). Then, the following result holds.

Theorem 2. *The predecessor-follower dynamics (27) are adaptively stabilizable via immersion and invariance (I&I). An I&I design is given by the adaptive law*

$$\dot{\hat{\tau}}_i(t) = -\frac{\partial\beta}{\partial\tilde{x}}A_\mathrm{m}\tilde{x}(t) - \frac{\partial\beta}{\partial\bar{x}}\left(A_\mathrm{m}\bar{x}(t) + G_\mathrm{m}\begin{bmatrix}a_{i-1}(t)\\ u_{i-1}(t)\end{bmatrix}\right), \tag{28}$$

with the control law

$$\Delta u_i(t) = u_i(t) - a_i(t) + \psi(t)\left(\hat{\tau}_i(t) + \beta(\tilde{x}(t),\bar{x}(t))\right), \tag{29}$$

with

$$\beta(\tilde{x}(t),\bar{x}(t)) = -\frac{\gamma}{\tau_\mathrm{m}}\tilde{a}_i(t)\left[u_i(t) - \frac{\tilde{a}_i(t)}{2} - \bar{a}_i(t)\right], \tag{30}$$

and $\gamma > 0$.

Proof. As the proof follows similar steps as the ones of Theorem 1, we focus on manifold attractivity and trajectory boundedness, for a system in the same form as (15), obtained from

$$\dot{\tilde{x}}(t) = A_\mathrm{m}\tilde{x}(t) + g\Delta\tilde{u}_i(t) - g\psi(t)\tau_i = A_\mathrm{m}\tilde{x}(t) + g\psi(t)z(t), \tag{31}$$

and from

$$\dot{z}(t) = \dot{\hat{\tau}}_i + \frac{\partial\beta}{\partial\tilde{x}}\dot{\tilde{x}}(t) + \frac{\partial\beta}{\partial\bar{x}}\dot{\bar{x}}(t), \tag{32}$$

with the adaptive law (28). The Lyapunov analysis, similar to Theorem 1, uses the Lyapunov function (18), and relies on the fact that β in (30) is such that

$$\frac{\partial\beta}{\partial\tilde{x}}g = -\frac{\gamma}{\tau_i}\psi. \tag{33}$$

We finally verify (5) by writing $e_i = \bar{e}_i + \tilde{e}_i$, where $\bar{e}_i$ converges to zero due to disturbance decoupling of the ideal closed loop (25) (with τ_m taken homogeneous for all vehicles), whereas $\tilde{e}_i$ converges to zero from the Lyapunov analysis. ∎

V. Comparison with Model Reference Adaptive Control

The dynamics (11) for the first protocol and (27) for the second protocol describe the tracking error between the actual closed-loop system and the target dynamics. As such, such dynamics are amenable to be used in a model reference adaptive control (MRAC) architecture with the reference model playing the role of the target dynamics. Indeed, the literature has reported adaptive longitudinal platooning protocol inspired by MRAC. For the first protocol an adaptive design was reported in [15], taking the form

$$\begin{aligned}\dot{\hat{\tau}}_i &= -\gamma B^\top P\tilde{x}\left(\frac{\theta_1}{\tau_\mathrm{m}}e_i + \frac{\theta_2}{\tau_\mathrm{m}}v_i - \left(\frac{h\theta_2}{\tau_\mathrm{m}} + \frac{1}{h}\right)a_i + \frac{1}{h}a_{i-1}\right)\\ u_i &= a_i + \left(\frac{\theta_1}{\tau_\mathrm{m}}e_i + \frac{\theta_2}{\tau_\mathrm{m}}v_i - \left(\frac{h\theta_2}{\tau_\mathrm{m}} + \frac{1}{h}\right)a_i + \frac{1}{h}a_{i-1}\right)\hat{\tau}_i,\end{aligned} \tag{34}$$

with $B^\top = [0\ 0\ h^{-1}]$, and P as in the Lyapunov equation (19). For the second protocol an adaptive design was reported in [13], taking the form

$$\dot{\hat{\tau}}_i = -\gamma B^\top P\tilde{x}\frac{u_i - a_i}{\tau_\mathrm{m}}, \quad \Delta u_i = u_i - a_i + \frac{u_i - a_i}{\tau_\mathrm{m}}\hat{\tau}_i, \tag{35}$$

with $B^\top = [0\ 0\ 1\ 0]$, P from its corresponding Lyapunov equation (in the same form as (19) but with A_m as in the target dynamics (25)). By comparing (12) with (34), and (28) with (35), it can be noted that the adaptive laws in the proposed I&I designs depart from existing MRAC designs. The difference between the I&I and the MRAC designs is even more evident in the control law: indeed, the MRAC designs adopt a certainty-equivalence control, that is, the unknown τ_i is directly replaced by $\hat{\tau}_i$. On the other hand, the I&I designs (13) and (29) depart from the certainty-equivalence control, due to the presence of the β term. Certainty-equivalence control in MRAC is the result of the use of a Lyapunov function of the form

$$W(\tilde{x},z) = \tilde{x}^\top\frac{P}{2}\tilde{x} + \tilde{\tau}^\top\frac{\rho}{2}\tilde{\tau}, \tag{36}$$

in which the first quadratic term is the same as in (18), while the second term is quadratic in $\tilde{\tau}_i = \hat{\tau}_i - \tau_i$, instead of being quadratic in the off-manifold variable z as in (18).

To verify the theoretical analysis, this section presents simulation results of a platoon with five vehicles (one leader indexed as 0 and four following vehicles indexed as 1, 2, 3, 4). All protocols, given for a predecessor-follower configuration, can be easily extended to platoons of arbitrary length, using vehicle pairs $(i-1, i)$. The initial conditions and vehicle time constants are shown in Table I.

TABLE I: Vehicle time constants and initial conditions

i	τ_i	$d_i(0)$	$v_i(0)$	$a_i(0)$
0	0.2	0	10	0
1	0.05	-2	12	0
2	0.1	-4	8	0
3	0.3	-6	11	0
4	0.25	-8	10	0

We simulate three scenarios:

1) non-adaptive scenario, which can be the first presented protocol (3) or the second presented one (4);
2) state-of-the-art MRAC version of the protocols above: (34) for the first protocol and (35) for the second one;
3) proposed I&I version of the protocols above: (12)-(13) for the first protocol and (28)-(29) for the second one.

We set the time headway $h = 0.7$ in all protocols. For the first protocol (3), we use $\theta_1 = 1$ and $\theta_2 = 1$. For the second

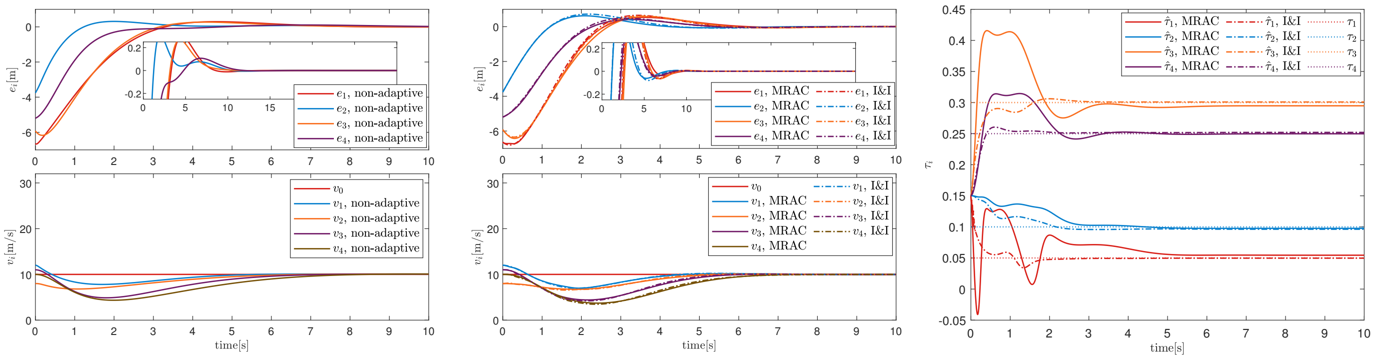

(a) Non-adaptive protocol (b) MRAC and I&I adaptive protocols (c) MRAC and I&I estimates of τ_i

Fig. 2: Comparisons between the non-adaptive protocol (3), and its MRAC and I&I adaptive versions. When the leading vehicle has constant velocity, all protocols achieve vanishing error. Note the smooth estimation behavior of the I&I design.

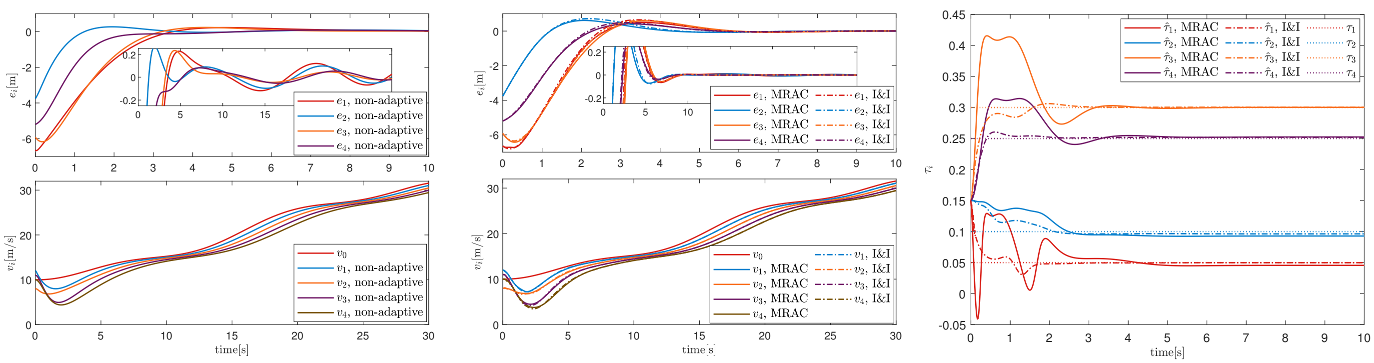

(a) Non-adaptive protocol (b) MRAC and I&I adaptive protocols (c) MRAC and I&I estimates of τ_i

Fig. 3: Comparisons between the non-adaptive protocol (3), and its MRAC and I&I adaptive version. In the absence of adaptation, poor knowledge of τ_i results in steady-state errors.

protocol (4), we use $\theta_1 = 0.75$ and $\theta_2 = 1.25$. To simulate incorrect knowledge of τ_i in the first protocol, we design it using $\tau_i = 0.2$ for all vehicles. For the MRAC designs, we use $Q = 0.7I$ and $\gamma = 0.3$ in the first protocol, and $Q = 0.25I$ and $\gamma = 0.3$ in the second protocol. Both the MRAC and I&I designs use a target time constant $\tau_{\mathrm{m}} = 0.5$, and γ in I&I is adjusted to be close to the combined adaptation gain of MRAC, by setting $\gamma = 0.04$ in the first protocol, and $\gamma = 0.09$ in the second protocol.

We start by considering the protocol (3) and its adaptive versions with $u_0 = 0$, implying that the leading vehicle moves at constant velocity. The spacing errors and velocity results are presented in Fig. 2a for the non-adaptive protocol, and in Fig. 2b for the adaptive ones. It can be seen that all protocols achieve vanishing spacing errors, meaning that the inter-vehicle distances converge to the desired ones. Fig. 2c shows that the estimation behavior in the I&I design is much smoother than the estimation behavior in the MRAC design. Then, when the leading vehicle proceeds with non-stationary behavior, e.g. $u_0 = \sin(0.1t) + 0.5\sin(0.5t)$, the non-adaptive protocol exhibits steady-state errors, with the inter-vehicle distances deviating from the desired ones, as shown in Fig. 3a: this is due to the incorrect knowledge of τ_i, which makes it impossible to achieve perfect disturbance decoupling. Fig. 3b and Fig. 3c show that, despite both adaptive protocols are able to attain vanishing spacing errors, the estimation behavior in the I&I design does not exhibit the overshooting behavior of the MRAC design.

We then consider the protocol (4) and its adaptive versions with the leading vehicle having $u_0 = \sin(0.1t) + 0.5\sin(0.5t)$. Fig. 4a shows steady-state errors: differently from the first protocol, such errors are due to the vehicles having heterogeneous time constants, while protocol (4) is designed for homogenous time constants. Because the MRAC and I&I are based on homogeneous target dynamics, they achieve vanishing errors, as shown in Fig. 4b and Fig. 4c. Once more, the estimation behavior in the I&I design does not exhibit the oscillating behavior of the MRAC design.

VI. Conclusions and Future Work

This work proposed new adaptive longitudinal platooning protocols in the framework of Immersion and Invariance (I&I). Such I&I designs have been directly compared to

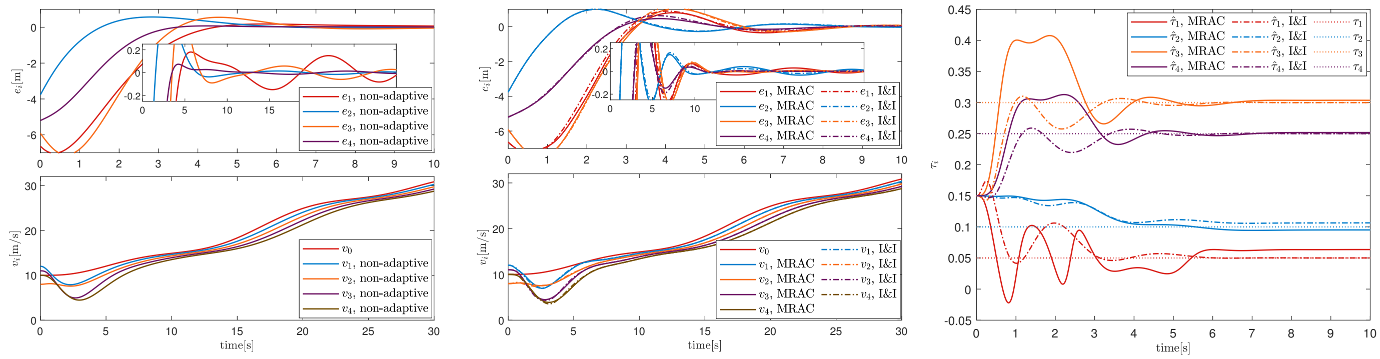

(a) Non-adaptive protocol (b) MRAC and I&I adaptive protocols (c) MRAC and I&I estimates of τ_i

Fig. 4: Comparisons between the non-adaptive protocol (4), and its MRAC and I&I adaptive version. In the absence of adaptation, steady-state errors result from the fact that the vehicles have heterogenous time constants.

state-of-the-art protocols relying on model reference adaptive control. Advantages have been discussed theoretically and via simulations. The I&I approach to adaptive longitudinal platooning is open to several extensions: it is of interest to consider nonlinearities in vehicle dynamics or reduced state measurements via output-feedback.

References

[1] K. C. Dey, L. Yan, X. Wang, Y. Wang, H. Shen, M. Chowdhury, L. Yu, C. Qiu, and V. Soundararaj, “A review of communication, driver characteristics, and controls aspects of cooperative adaptive cruise control CACC,” *IEEE Transactions on Intelligent Transportation Systems*, vol. 17, no. 2, pp. 491–509, 2016.

[2] E. Kayacan, “Multiobjective H_∞ control for string stability of cooperative adaptive cruise control systems,” *IEEE Transactions on Intelligent Vehicles*, vol. 2, no. 1, pp. 52–61, 2017.

[3] S. Feng, Z. Song, Z. Li, Y. Zhang, and L. Li, “Robust platoon control in mixed traffic flow based on tube model predictive control,” *IEEE Transactions on Intelligent Vehicles*, vol. 6, no. 4, pp. 711–722, 2021.

[4] J. Ploeg, E. Semsar-Kazerooni, G. Lijster, N. van de Wouw, and H. Nijmeijer, “Graceful degradation of cooperative adaptive cruise control,” *IEEE Transactions on Intelligent Transportation Systems*, vol. 16, no. 1, pp. 488–497, 2015.

[5] J. Ploeg, N. van de Wouw, and H. Nijmeijer, “$\mathscr{L}_p$ string stability of cascaded systems: Application to vehicle platooning,” *IEEE Transactions on Control Systems Technology*, vol. 22, no. 2, pp. 786–793, 2014.

[6] F. Acciani, P. Frasca, G. Heijenk, and A. A. Stoorvogel, “Stochastic string stability of vehicle platoons via cooperative adaptive cruise control with lossy communication,” *IEEE Transactions on Intelligent Transportation Systems*, vol. 23, no. 8, pp. 10 912–10 922, 2022.

[7] V. S. Dolk, J. Ploeg, and W. P. M. H. Heemels, “Event-triggered control for string-stable vehicle platooning,” *IEEE Transactions on Intelligent Transportation Systems*, vol. 18, no. 12, pp. 3486–3500, 2017.

[8] P. Wijnbergen and B. Besselink, “Existence of decentralized controllers for vehicle platoons: On the role of spacing policies and available measurements,” *Systems & Control Letters*, vol. 145, p. 104796, 2020.

[9] P. Wijnbergen, M. Jeeninga, and B. Besselink, “Nonlinear spacing policies for vehicle platoons: A geometric approach to decentralized control,” *Systems & Control Letters*, vol. 153, p. 104954, 2021.

[10] D. Liu, S. Baldi, and S. Hirche, “Collision avoidance in longitudinal platooning: Graceful degradation and adaptive designs,” *IEEE Control Systems Letters*, vol. 7, pp. 1694–1699, 2023.

[11] H. Rezaee, T. Parisini, and M. M. Polycarpou, “Leaderless cooperative adaptive cruise control based on the constant time-gap spacing policy,” *IEEE Transactions on Automatic Control*, vol. 69, no. 1, pp. 659–666, 2024.

[12] S. Xie, J. Hu, Z. Ding, and F. Arvin, “Cooperative adaptive cruise control for connected autonomous vehicles using spring damping energy model,” *IEEE Transactions on Vehicular Technology*, vol. 72, no. 3, pp. 2974–2987, 2023.

[13] Y. A. Harfouch, S. Yuan, and S. Baldi, “An adaptive switched control approach to heterogeneous platooning with intervehicle communication losses,” *IEEE Transactions on Control of Network Systems*, vol. 5, no. 3, pp. 1434–1444, 2018.

[14] S. Baldi, D. Liu, V. Jain, and W. Yu, “Establishing platoons of bidirectional cooperative vehicles with engine limits and uncertain dynamics,” *IEEE Transactions on Intelligent Transportation Systems*, vol. 22, no. 5, pp. 2679–2691, 2021.

[15] D. Liu, B. Besselink, S. Baldi, W. Yu, and H. L. Trentelman, “An adaptive disturbance decoupling perspective to longitudinal platooning,” *IEEE Control Systems Letters*, vol. 6, pp. 668–673, 2022.

[16] ——, “Output-feedback design of longitudinal platooning with adaptive disturbance decoupling,” *IEEE Control Systems Letters*, vol. 6, pp. 3104–3109, 2022.

[17] A. Astolfi and R. Ortega, “Immersion and invariance: a new tool for stabilization and adaptive control of nonlinear systems,” *IEEE Transactions on Automatic Control*, vol. 48, no. 4, pp. 590–606, 2003.

[18] A. Venkatraman, R. Ortega, I. Sarras, and A. van der Schaft, “Speed observation and position feedback stabilization of partially linearizable mechanical systems,” *IEEE Transactions on Automatic Control*, vol. 55, no. 5, pp. 1059–1074, 2010.

[19] D. Carnevale and A. Astolfi, “Semi-global multi-frequency estimation in the presence of deadzone and saturation,” *IEEE Transactions on Automatic Control*, vol. 59, no. 7, pp. 1913–1918, 2014.

[20] A. Astolfi, L. Hsu, M. Netto, and R. Ortega, “Two solutions to the adaptive visual servoing problem,” *IEEE Transactions on Robotics and Automation*, vol. 18, no. 3, pp. 387–392, 2002.

[21] L. Wang, F. Forni, R. Ortega, and H. Su, “Immersion and invariance stabilization of nonlinear systems: A horizontal contraction approach,” in *54th IEEE Conference on Decision and Control (CDC)*, 2015, pp. 3093–3097.

[22] L. Wang and C. M. Kellett, “Adaptive tracking control via immersion and invariance: An (i)ISS perspective,” in *58th IEEE Conference on Decision and Control (CDC)*, 2019, pp. 7019–7024.

[23] R. Ortega, B. Yi, J. G. Romero, and A. Astolfi, “Orbital stabilization of nonlinear systems via the immersion and invariance technique,” *International Journal of Robust and Nonlinear Control*, vol. 30, no. 5, pp. 1850–1871, 2020.

[24] D. Liu, B. Besselink, S. Baldi, W. Yu, and H. L. Trentelman, “On structural and safety properties of head-to-tail string stability in mixed platoons,” *IEEE Transactions on Intelligent Transportation Systems*, vol. 24, no. 6, pp. 6614–6626, 2023.

[25] D. Hajdu, J. I. Ge, T. Insperger, and G. Orosz, “Robust design of connected cruise control among human-driven vehicles,” *IEEE Transactions on Intelligent Transportation Systems*, vol. 21, no. 2, pp. 749–761, 2020.